Mass and Thermal Transport Analysis of Oscillating Flow with Absorbent Polymers

Kenneth M. Kalumuck, Sankar Prabhukumar, Clinton E. Brown, and Georges L. Chahine
DYNAFLOW, Inc., Fulton, MD 20759

A new concept for removing toxic gases with respirator applications based on inhalation and exhalation through absorbent polymer-lined tubes was studied. The two-way oscillatory flow through the respirator element enables capture and expulsion of toxic vapors, which is not feasible with activated charcoal because of the adverse effect of moist breath on the charcoal efficiency. To study the influence of various material, design and operating parameters on the performance of such a respirator, a numerical model that solves the governing equations of mass and heat transport in an oscillatory flow through an absorbent polymer-lined tube was developed and utilized with experimentally measured property data. Factors investigated include respirator element geometry, polymer and toxic vapor characteristics, and flowthrough speed. Results show a large delay in toxic gas penetration over that obtained by conventional one-way flow, and define the importance of partition coefficient, flow passage size, and length and velocity. Results are compared with data from simulated breathing experiments.

Introduction

This paper presents results of research carried out in an effort to improve workplace respirators by reductions in size and weight. The concept studied involves alternating flow (inhaling and exhaling) through the filter material, allowing for ejection of a large fraction of the toxic material captured by the filter during intake. Systems using activated charcoal currently in use are valved because the charcoal degrades in adsorptive performance if exposed to humid breath on exhaling. Thus, for two-way flow it is important to find filter materials that are not degraded by the presence of water vapor at concentrations found in human breath. To this end, the project concentrated on polymeric materials that *absorb* rather than *adsorb* toxic gases.

To study the effects of various designs, material properties, and operating parameters, a numerical model to simulate the mass and thermal transport in alternating flow with absorbent polymers was developed. The model was used both for parametric studies and to provide guidance in planning and carrying out an experimental program. Analytical studies were done for the case of polymers perforated with fine parallel holes. In this article, the differential equations representing the mass and heat transfer within the air channels and the polymer are first presented, followed by a description of the numerical implementation of the model. Results of the parametric study and comparison with experimental data are presented. The results illustrate the highly nonlinear behavior of the concentrations with the various parameters. Implications of these results for the design of respirators are discussed. Details of the experimental program can be found in Brown et al. (1996a,b). In addition, the model has been utilized in a related study of the effects of large temperature variations in a gas concentration system based on absorption and desorption with polymers (Kalumuck et. al., 1994).

A wide variety of toxic vapors are present in industrial work places either on a normal operating basis or under an emergency situation, such as due to a failure resulting in a sudden release or to leakage. Exposure limits to various substances are given by the American Conference of Government Hygienists (1989). It is desirable to make respirators as light, compact, and long-lived as possible. This would increase the comfort to the user, thereby making it easier to work while wearing a respirator and decreasing user fatigue. In addition, the pressure drop across the respirator should be minimal, both to make breathing easy and to minimize leakage across the face seal. The novel technique that we have developed to

Correspondence concerning this article should be addressed to K. M. Kalumuck.

achieve these objectives is to construct the respirator of tubes lined with a polymer that absorbs toxic gases. A respirator filter would consist of a large number of these small tubes arranged in a parallel bundle. Alternatively, the absorbent polymeric material may have fine pores whose passage length is much larger than the pore diameter. Breathing both in and out through these tubes sets up an oscillatory flow. On inhalation, the toxic gas is absorbed by the polymer. On exhalation, the toxic gas is desorbed into the initially contaminant free out-breath and expelled out of the respirator. Due to the physics of the mass transfer processes and the typical breathing cycle, not all of the gas is expelled from the respirator and a gradual increase in gas held in the polymer occurs, which ultimately determines the effective life of the respirator element.

Activated charcoal is currently used in many respirators, gas masks, and air purification systems because of its excellent adsorption characteristics for many toxic gases. (See, for example, Tollen, 1968 or Yaws, et al., 1995). It is known, however, that the presence of water vapor even at normal values of atmospheric concentration can sharply reduce the capacity of activated charcoal for gas adsorption. It is for this reason that charcoal canisters should be sealed from air contact until they are needed. Absorbent polymers are not subject to these interference effects, as discussed below.

Alternating flow filters using wall coatings of *absorbent* polymeric materials should be of greatest interest for respirators because the sorption process is much less sensitive to water vapor and other interferences than *adsorption* processes. In absorption, molecules of the substance being absorbed enter into a solution within the absorbing media. In adsorption processes, the molecules being absorbed adhere to the surface of the adsorbing media. Polymers that have extremely high partition coefficients for high-boiling-point vapors can thereby provide highly absorptive surface coatings. Grate et al. (1988) provide partition-coefficient data for a number of polymer/gas combinations.

Analysis of the Mass and Thermal Transport

Basic assumptions and simplifications

In order to study the influence of various parameters, a model was formulated for the case of a respirator consisting of an array of small-diameter cylindrical perforations in a polymer of some finite thickness. Such a configuration allows for an approximate computation of the mass and heat transfer between the air in the channels and the solid polymer. If we consider an arrangement of holes whose centers are arranged in an equilateral triangular grid, the respirator can be modeled as consisting of a large number of identical cells of hexagonal cross section in whose center is an air channel of circular cross section. The amount of polymer in each cell surrounding a channel can be written:

$$\text{Polymer Volume} = (2\sqrt{3}\,z^2 - \pi R_a^2)L, \tag{1}$$

where z is one-half the center-to-center hole-spacing distance; L is the channel length; and R_a is the channel radius. The first term in this expression is the area of the hexagonal cell, while the second is simply the channel cross-sectional area. To simplify the calculation with small error we consider the problem to be axially symmetric and introduce an effective radius R_p such that the polymer volume included in a cell of circular cross section with radius R_p surrounding the air channel of radius R_a is the same as that in the hexagonal cell. The defined radius, R_p, is given by the relation

$$R_p = \left[\frac{2\sqrt{3}\,z^2}{\pi}\right]^{0.5}. \tag{2}$$

The flow of air into this system is characterized by two mean velocities, the mean velocity in the air channel, U_{mean}, and the mean apparent superficial velocity, U_A. These velocities are related by the expression

$$U_{\text{mean}}/U_A = R_p^2/R_a^2. \tag{3}$$

Other simplifications of the analysis are the assumption that thermal conductivity and specific heat of the polymer are independent of toxic-gas concentration. However, we do include variation with the temperature of the properties governing the absorption, desorption, and diffusion of the contaminant gas. The solubility and partition coefficient are particularly sensitive to temperature. For example, in Hagel et al. (1977), it was found that the solubility and partition coefficients for various polymers can vary by more than factor of 3 over the temperature range 30–50°C. We have found the same trends in our measurements. Thus the instantaneous temperature distribution in the respirator could be important to properly model the absorption, desorption, and transport of the contaminant gas. To this end we developed a coupled heat and mass-transfer model to predict system performance. The model solves the heat and mass-transport equations for fully developed laminar flow (the Reynolds number based on mean air flow velocity and tube diameter is of the order of 1–2 for the typical conditions considered) in polymer tubes. The heat and mass-transfer transport relations are coupled due to the temperature dependence of various properties, as described below.

The parameters of the model problem (Figure 1) include:

(a) The polymer/gas pair partition coefficient, K:

(b) The mass-diffusion coefficients of the gas in the air and in the polymer, D_a, D_p.

(c) The physical dimensions: tube radius, length and radius of the outer boundary of the polymer layer, R_a, L, R_p.

(d) The axial flow velocity, U.

(e) The concentrations of gas in the air and polymer, C_a, C_p.

(f) The air and polymer temperatures, T_a, T_p.

(g) The air and polymer densities, ρ_a, ρ_p.

(h) The air and polymer thermal conductivities and specific heats, k_a, k_p, $c_{p,a}$, $c_{p,p}$.

Typical values of these parameters used in the computations below are given in Table 1, and are also noted on the individual figures that summarize the model predictions.

The axial velocity distribution in the channel can be written as

$$U(x,r,t) = U_{\text{mean}} \cdot f_1(r) \cdot f_2(t) \cdot f_3(x,t), \tag{4}$$

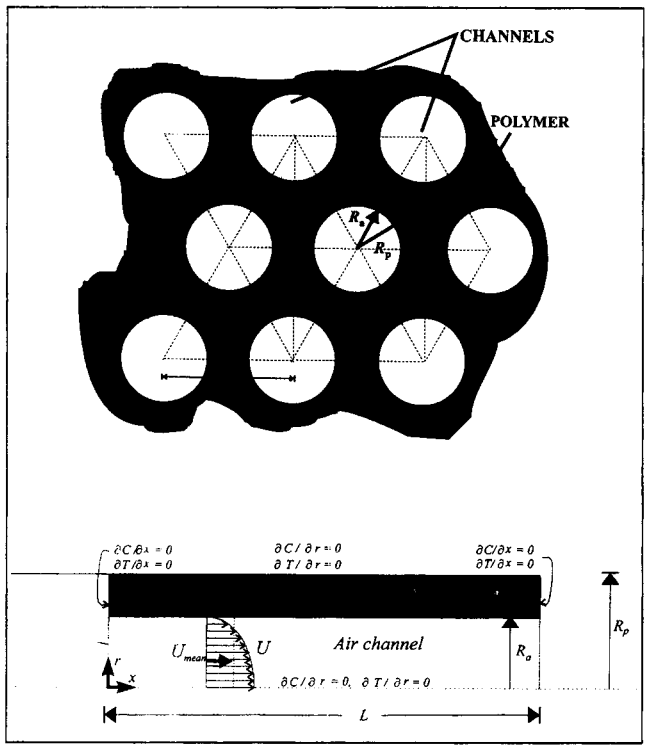

Figure 1. Ideal respirator with parallel cylindrical holes (top) and of computational model domain (bottom).

where U_{mean} is the uniform velocity entering the tube averaged over τ, one half a breathing cycle; x and r are axial and radial coordinates; and t is time. Here,

$$f_1 = 2\left(1 - \frac{r^2}{R_{a^2}}\right), \tag{5}$$

$$f_2 = \frac{\pi}{2} \sin\left(\pi \frac{t}{\tau}\right), \tag{6}$$

$$f_3 = \frac{T_a(x,0,t)}{T_a(0,0,0)}. \tag{7}$$

Equation 5 represents a laminar and fully developed flow. This assumption is justified, given the Reynolds numbers considered in the calculations. Equation 6 is an approximation to human breathing cycles. Typical values for τ would be 2.5 s for in breath and 3.5 s for out breath. Equation 7 allows for mean density change along the tube, produced by the axial temperature variation at the tube center line $T_a(x,0,t)$ (which approximates well the bulk mean temperature within the channel at any station x, since as will be seen later, radial temperature gradients in air are negligible). T_a is the air temperature entering the tube taken to be constant with time and equal to its value at $t = 0$, $T_a(0,0,0)$. The velocity distribution within the tube is then

$$U(x,r,t) = \pi U_{\text{mean}} \sin \frac{\pi t}{\tau} \left(1 - \frac{r^2}{R^2}\right) \frac{T_a(x,0,t)}{T_a(0,0,0)}. \tag{8}$$

Table 1. Values of Physical Constants and Parameters Used in Numerical Simulations

Physical Constant or Parameter	Values Used
K	400–122,000*
D_a	0.038–0.075 cm^2/s
D_p	10^{-8}–5×10^{-7} cm^2/s
R_a	0.13–0.79 mm
R_p/R_a	1.38–2.44
L	1.27–5.08 cm
U_{mean}	3.7–24.4 cm/s
τ	3 s

*Results for K as low as 25 are presented in Brown, e.t. al. (1996a).

Thermal transport

The thermal transport equations can then be expressed as

$$\rho_a c_{p,a} \frac{\partial T_a}{\partial t} = \frac{\partial k_a}{\partial T_a} \nabla T_a + k_a \nabla^2 T_a - \rho_a U c_{p,a} \frac{\partial T_a}{\partial x}, \tag{9}$$

$$\rho_p c_{p,p} \frac{\partial T_p}{\partial t} = \frac{\partial k_p}{\partial T_p} \nabla T_p + k_p \nabla^2 T_p, \tag{10}$$

where subscripts a and p refer to the air and polymer, respectively. In these equations, water-vapor flux is not explicitly shown and is made part of the air flux, since we will be considering polymeric materials whose properties are not affected by the presence of water vapor. At the polymer/air interface ($r = R_a$), the conditions are continuity of heat flux and of temperature

$$k_a \frac{\partial T_a}{\partial r} + h_{\text{sol}} D_a \frac{\partial C_a}{\partial r} = k_p \frac{\partial T_p}{\partial r}, \tag{11}$$

$$T_a = T_p, \tag{12}$$

where h_{sol} is the heat of solution for the gas forming a solution with the polymer. Selection of the boundary condition at the outer edge of the polymer depends on the actual physical geometry as previously discussed. In the multitube respirator being considered, the boundary between the polymer layers associated with adjacent tubes can be modeled as having no net transfer across them, since all tubes are taken as being identical. Thus the boundary condition at $r = R_p$ is

$$\frac{\partial T_p}{\partial r} = 0. \tag{13}$$

The inner and outer faces of the polymer respirator are in contact with atmospheric air and with the region of air near the mouth. The heat transfer across these boundaries is negligible, as it must occur through radiation or conduction, since the air velocity at these locations is an order of magnitude smaller than in the individual channels, and the boundary condition can be approximated as being adiabatic:

$$\frac{\partial T_p}{\partial x} = 0; \qquad x = 0, L. \tag{14}$$

At the air channel entrance ($x = 0$) during in-breath, the temperature is equal to atmospheric temperature. During out-breath, the air temperature at the mouth ($x = L$) is equal to that of exhaled air. The outflow conditions for both the forward and reverse flows are taken to be

$$\frac{\partial T_a}{\partial x} = 0 \quad \text{at} \quad x = L, \quad U > 0;$$

$$\text{and} \quad x = 0, \quad U < 0. \quad (15)$$

Mass transport

In situations where the bulk fluid density ρ_a is not constant, such as will be the case in the air channel with varying temperature, it is convenient to express the equations in terms of a mass fraction C_a^*, where

$$C_a^* = \frac{C_a}{\rho_a}. \quad (16)$$

Due to a very low coefficient of thermal expansion (e.g., for dimethyl silicone (DMS) the density variation over the temperature range 17 to 37°C is less than 1% of its mean value), the polymer density is taken as constant. The differential equations governing the mass transfer in axisymmetric geometry are then

$$\rho_a \frac{\partial C_a^*}{\partial t} = \frac{1}{r}\frac{\partial}{\partial r}\left(r\rho_a D_a \frac{\partial C_a^*}{\partial r}\right) + \frac{\partial}{\partial x}\left(\rho_a D_a \frac{\partial C_a^*}{\partial x}\right) - \rho_a U(x,r,t)\frac{\partial C_a^*}{\partial x}, \quad (17)$$

$$\frac{\partial C_p}{\partial t} = \frac{1}{r}\frac{\partial}{\partial r}\left(rD_p \frac{\partial C_p}{\partial r}\right) + \frac{\partial}{\partial x}\left(D_p \frac{\partial C_p}{\partial x}\right). \quad (18)$$

The boundary conditions at the polymer/air interface are

$$D_a \frac{\partial C_a}{\partial r} = D_p \frac{\partial C_p}{\partial r} \quad \text{at} \quad r = R_a, \quad (19)$$

$$C_p = KC_a \quad \text{at} \quad r = R_a. \quad (20)$$

At the polymer outer boundaries, by the same argument used for the thermal problem:

$$D_p \frac{\partial C_p}{\partial r} = 0 \quad \text{at} \quad r = R_p; \quad x = 0, L. \quad (21)$$

In the air channel, at in-flow, the upstream concentration is equal to the initial concentration, and on reverse flow, the return concentration is zero. The outflow conditions for both the forward and reverse flows are taken to be $(\partial C_a/\partial x) = 0$, at $x = L$, $U > 0$; and $x = 0$, $U < 0$.

Numerical implementation

An alternating direction implicit (ADI) finite difference scheme (Peyret and Taylor, 1983) was developed to solve the problem previously outlined. The numerical model includes:

(a) Unsteady diffusion and convection of both heat and mass

(b) Simultaneous heat and mass transfer with an imposed time-dependent temperature boundary condition and velocity profile

(c) Temperature-dependent air and polymer properties

(d) Heat of solution effects (heating/cooling effects due to mass absorption/desorption).

The ADI was implemented utilizing second-order centered differences in space and first-order forward differences in time. Second-order accurate boundary conditions were employed except at the air/polymer interface where, for increased accuracy, a fourth-order scheme was employed. The ADI was chosen over other schemes for reasons of stability and speed (Peyret and Taylor, 1983). For the problem at hand, which involves a combination of diffusion, convection, and interface boundary conditions that couple the polymer and the air channel, it was found that a criterion for stability established a maximum allowable time step.

A series of stability and convergence studies were performed, which led to the following stability criterion:

$$D\Delta t/(\Delta r)^2 \le 2, \quad (22)$$

where Δr and Δt are the space and time step sizes. This is a factor of 8 increase in the maximum allowable time step over that of an explicit method. A detailed convergence analysis was performed to establish the sensitivity of the code to space and time discretization size. Properties of the polymer gas pair, DMS and dimethyl methyl phosphonate (DMMP), that we measured were used. It was found that results were very sensitive to resolution of the behavior at the air/polymer interface. The temperature and concentration gradients must be adequately resolved to accurately compute the heat and mass-transfer across this interface. The fourth-order difference scheme used at the interface was found to achieve a high degree of accuracy with a reasonable discretization.

Figures 2–5 present results of a convergence study. Shown are plots of the axial and radial nondimensional concentration (C/C_o) distributions. All figures are taken at the end of the first forward-flow (in-breath) cycle. *The concentration inside the polymer is normalized using the partition coefficient, K, to enable the concentrations in the air and the polymer to be displayed on the same scale.* In Figures 2 and 3, the discretizations in the r-direction and in time were held constant, while the axial discretization was varied from 75 grid points (nx) down to 5. These figures show the insensitivity of the results to the axial discretization. In Figures 4 and 5, the radial and temporal discretizations were varied. The axial discretization was also varied to maintain the same grid aspect ratio. It was not possible to analyze the discretization in the r-direction and in time separately because of the stability criterion discussed earlier. Stability considerations forced a decrease in the time step with a decrease in the grid size. The time step utilized represents the maximum allowable for a given radial discretization. As can be seen, the results are more sensitive to the radial discretization than to the axial discretization. Based on these results a discretization of 20 points in both the axial and radial directions with at time step of $5 \cdot 10^{-3}$ s was chosen as adequate for providing a converged solution.

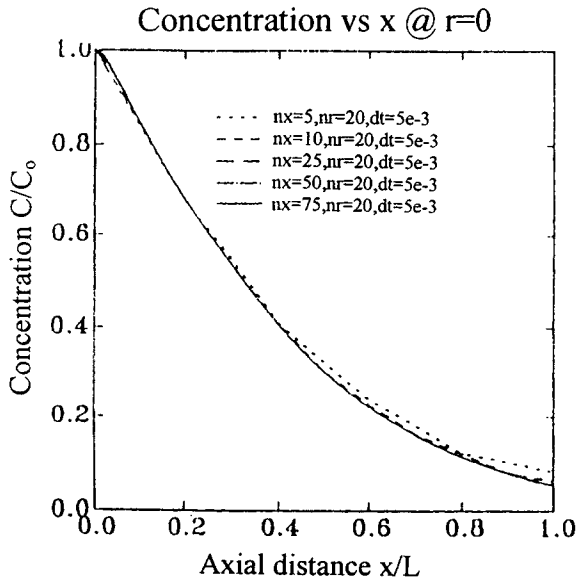

Figure 2. Convergence of axial concentration distribution with axial discretization (*nx*).

Time step (*dt*), and radial discretization (*nr*) kept constant.

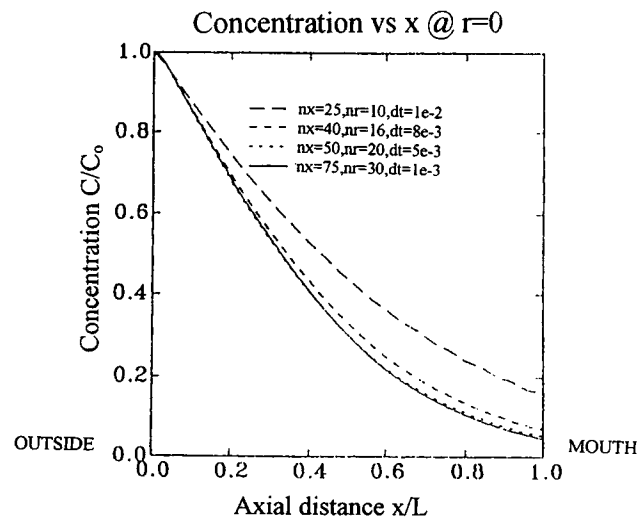

Figure 4. Convergence of axial concentration distribution with radial discretization.

Ratio of axial to radial discretization kept constant. Time step taken to be largest allowed for each discretization.

Limiting solutions for infinitesimal hole size

It is of interest to determine the absorber performance that could be achieved by reducing the hole sizes in the polymer to zero while keeping the ratio R_p/R_a constant. This would provide for maximum (in fact infinite) radial mass and heat transfer in the air and polymer. It thus represents an upper bound on the performance that could be achieved by decreasing air passage size. The problem is then one-dimensional in space—a function only of position x. A numerical analysis of this case was made for the case of constant diffusivity and partition coefficient. The assumed small (zero) scale of the lateral dimensions ensures that the air and polymer concentrations will be independent of r. The differential equation to be solved becomes:

$$\frac{\partial C}{\partial t} = \left[D_p + \frac{D_a}{K\left(\frac{R_p^2}{R_a^2} - 1\right)} \right] \frac{\partial^2 C}{\partial x^2} - \frac{U_m}{K\left(\frac{R_p^2}{R_a^2} - 1\right)} \frac{\partial C}{\partial x}. \quad (23)$$

Boundary conditions at $x = 0$ and $x = L$ were the same as those used for the complete problem discussed earlier.

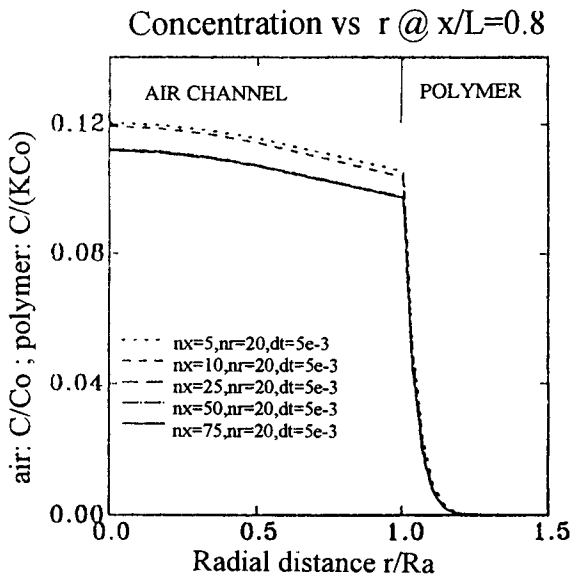

Figure 3. Convergence of radial concentration distribution with axial discretization (*nx*).

Time step (*dt*), and radial discretization (*nr*) kept constant. $r/R_a = 1$ is the polymer/air interface.

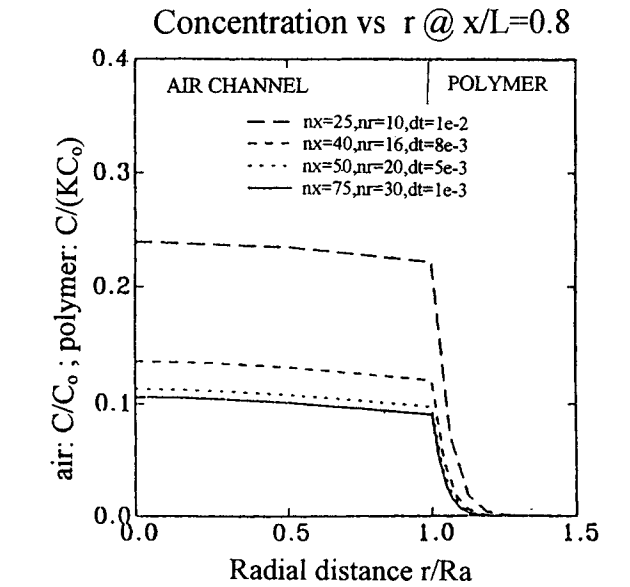

Figure 5. Convergence of radial concentration distribution with radial discretization.

Ratio of axial to radial discretization kept constant. Time step taken to be largest allowed for each discretization.

Results and Discussion

Calculations were carried out to obtain the estimated mean concentration exiting the tubes as a function of time. To illustrate the effect of the several variables, runs were made varying only a single variable over what were considered reasonable values for respirator design.

Influence of properties

The variable of greatest interest is the partition coefficient, as this value for various polymer/gas pairs can vary from about 10^2 to 10^6; the lower values corresponding to gases having very high vapor pressures at room temperatures, with the higher values corresponding to gases with low room-temperature vapor pressures. The effect of partition coefficient variation is shown in Figure 6, which demonstrates the strong influence of K on performance. For example, at one hour of breathing, a 200-fold increase in K (from 400 to 80,000) results in a decrease in concentration at the mouth by five orders of magnitude. The other parameters held constant are also shown on the figure. For low K values the system arrives at an equilibrium state for C_m/C_o (where C_m is the bulk average concentration over a cycle) in a quite short time, but for the large K values, equilibrium is greatly delayed. For respirator use, times less than an hour would be of interest for emergency use; for industrial use, 2 to 8 hours would be desired. For larger values of the channel length, lower apparent velocities, and smaller channel radii, the time to reach breakthrough values will be increased, as will be shown in subsequent figures. The value of K of 80,000 shown in the figure may indeed be obtained for polymers absorbing low vapor-pressure toxic compounds, and the geometries shown would allow for breakthrough times as long as 10 h for a C_m/C_o value of 0.01 and $4\frac{1}{2}$ h for a C_m/C_o values of 0.001.

Diffusion in the polymer and air also play important roles in the performance of the respirator system. Figure 7 shows the result of variations in the polymer gas diffusivity that exhibit decreased concentrations with increased diffusivity, as the gas can more rapidly diffuse to the outer reaches of the polymer. Polymer diffusivities are not a design choice except by choice of the polymer. Figure 8 demonstrates for the parameters shown the effect of a factor of 2 change in the diffusion coefficient of the toxic gas in air. As the diffusivity in the air decreases, increased resistance to diffusion across the channel impairs absorption by the polymer.

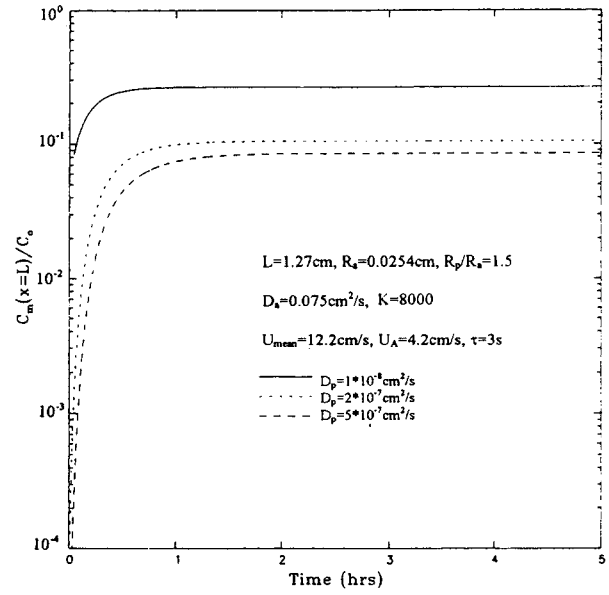

Figure 7. Variation of C_m/C_o with polymer diffusivity.

The polymer can take in more gas (C_m/C_o decreases) as the polymer diffusivity increases.

Influence of geometry

Variation of the length and diameter of the passages is predicted to have a major effect on the absorptive time histo-

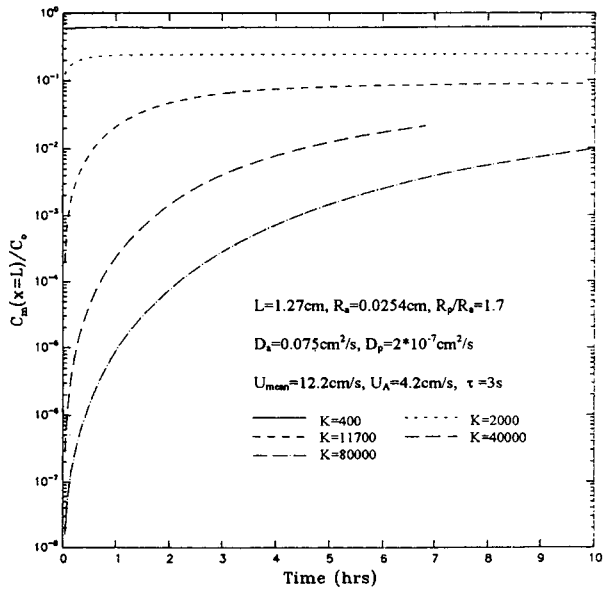

Figure 6. Variation of C_m/C_o with partition coefficient.

C_m/C_o decreases as K increases.

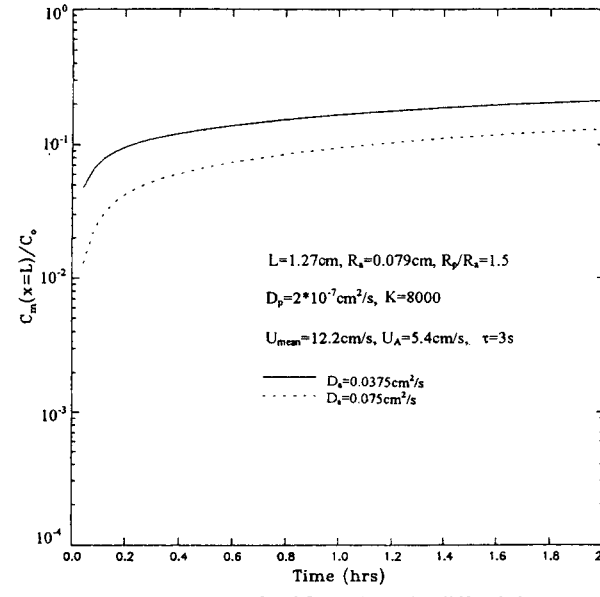

Figure 8. Variation of C_m/C_o with air diffusivity.

The polymer takes in more gas (C_m/C_o decreases) as the air diffusivity increases.

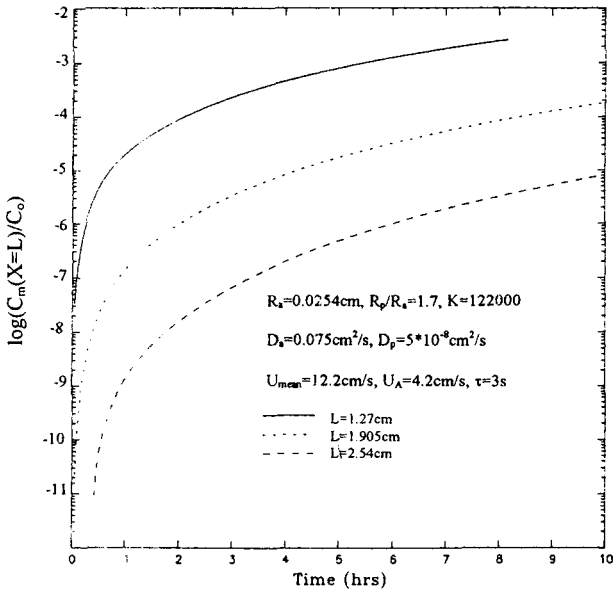

Figure 9. Variation of C_m/C_o with channel length, L.

As L increases, more polymer and time are available for gas transport and absorption.

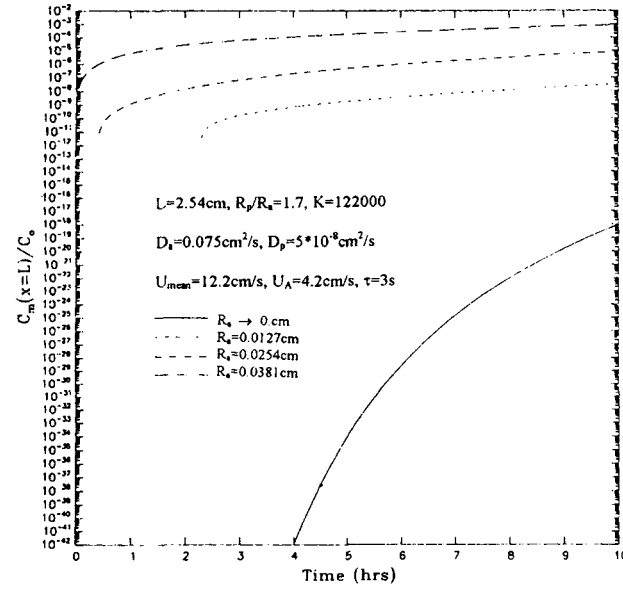

Figure 10. Variation of C_m/C_o with channel radius, R_a.

As R_a decreases, there is less gas per unit surface area of the polymer, allowing the polymer to absorb much more readily.

ries. Figure 9 shows the result of length variation. Doubling the length doubles the amount of polymer involved in the mass exchange, and this in turn provides a more than proportional reduction in the exiting concentration at any given time (e.g., a factor of 100 after 4 h), indicating that performance per unit weight of polymer increases with length. Decreasing the channel radius, as shown in Figure 10, also produces marked reductions in exiting concentrations due to the decrease in radial distance for diffusion to occur.

Influence of velocity

Figure 11 illustrates the effect of mean velocity in the channels showing a favorable effect of reductions in velocity. Reduction in velocity by a factor of 2 is seen to improve predicted performance (decrease concentration) by an order of magnitude or more. This effect is most pronounced at short times. A decrease in velocity would need to be accompanied by an increase in the total cross-sectional area for flow that could be accomplished by an increase in the number of channels, which would, keeping other variables constant, increase the size of the respirator. However, due to the nonlinear effects shown here, the increase in size associated with channel velocity reduction is more than compensated for by performance improvement.

Concentration distributions

Figure 12 presents the predicted concentrations along the channel axis as a function of time. The concave shape of the curves gradually approaches at long times a nearly linear variation from the entrance to the exit of the channels. Figure 13 shows timewise variations in concentration at three radial positions at an axial station. It can be seen that the oscillations in concentration die out rapidly with radial distance into the polymer. It is not surprising that this is so, as a one-dimensional analysis of a sinusoidally varying concentration at the air/polymer interface indicates that the amplitude of the diffusional oscillations should die out in the polymer according to the simple relation (White, 1974):

$$C(y) = C_B \cdot e^{-\sqrt{\frac{\pi}{2\tau D_p}}\,y}, \qquad (24)$$

where C_B is the amplitude of the concentration at the surface and y is the distance from the surface into the polymer.

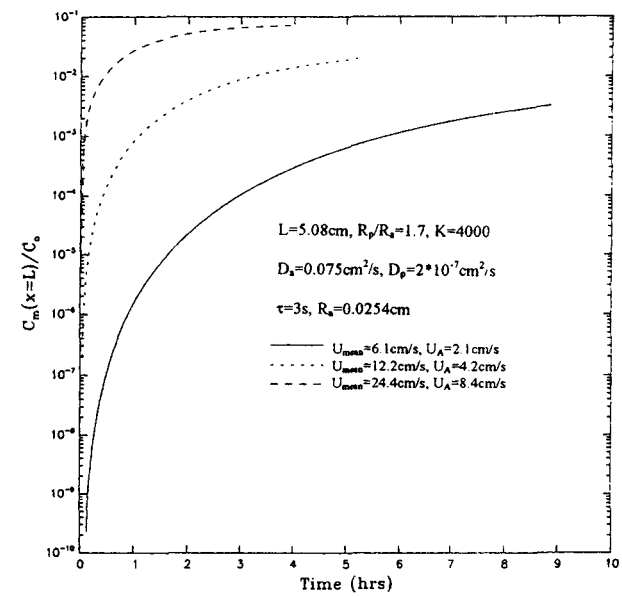

Figure 11. Variation of C_m/C_o with air mean velocity, U_{mean}.

As U_{mean} decreases, less axial transport is allowed and more radial transport and absorption is possible.

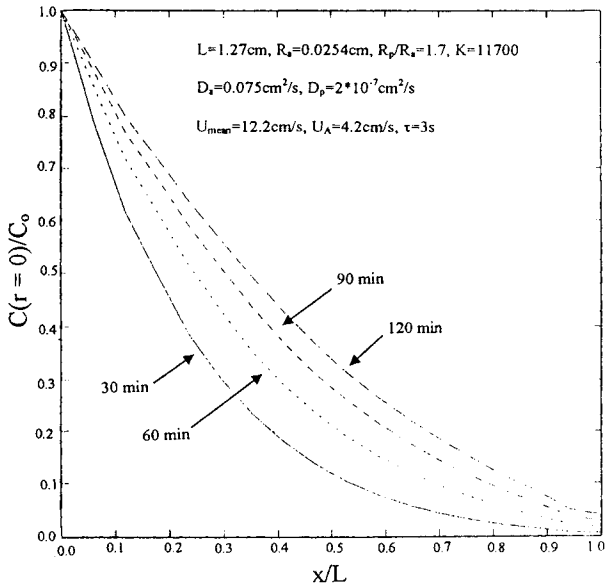

Figure 12. Predicted concentration distributions along the tube length at selected times.

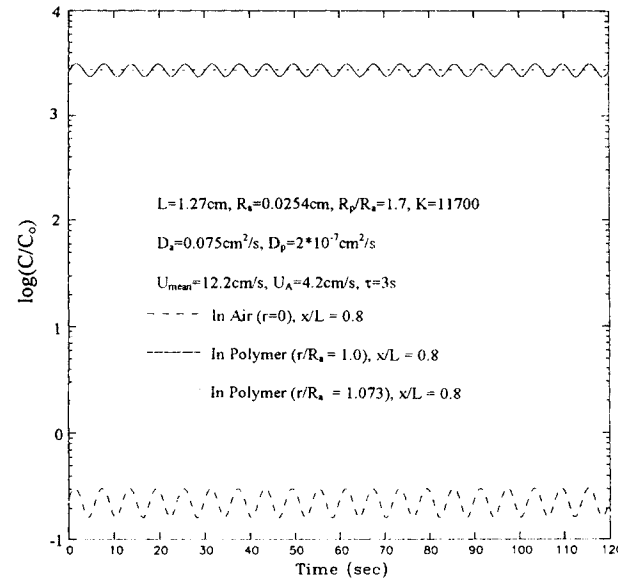

Figure 13. Predicted cyclic concentrations after 1 h of breathing.

Considering a typical breathing period, 2τ, of 6 s and a diffusion coefficient of say 10^{-7} cm^2/s, the preceding relation shows that the penetration into the polymer to a concentration level of 1% of C_B would be only 0.0018 cm, which corresponds to a value in Figure 13 of $r/R_a = 1.073$. The small fluctuations at this depth would not be observable at the scale of the figure, and the steady level shown here is the result of a continuous diffusion from the time mean values in the air channel. Thus, as time proceeds, concentrations in the outer regions of polymer grow steadily to reach an equilibrium value dependent only on distance along the channel.

Temperature distributions

The effects of temperature variation in the respirator, which lead to variation in property values, were also examined. The diffusion of heat in the polymer is much more rapid than the diffusion of the toxic gas contaminant (e.g., for DMS, the thermal diffusivity, $k_p/\rho_p c_{p,p} \approx 10^{-3}$ cm^2/s, while the diffusivity for DMMP in DMS is $D_p \approx 2\times10^{-7}$ cm^2/s). Consequently, the temperatures in the system reach equilibrium values relatively quickly, as can be seen in Figure 14. The calculations here are for poly epichlorohydrin (PECH). They indicate an approach to an equilibrium state after only 12.5 min of breathing. There is, however, a very small temperature swing at any point in the channel during a breathing cycle, as shown in Figure 15. For breath exhausting at 35°C and ambient air temperature of 20°C, the internal temporal variation at any point is less than about three-quarters of a degree centigrade. The resulting temperature distribution after only a short time shows that the air breathed would be at a temperature very close to body temperature, 37°C.

The effect of the temperature variation along the channel is illustrated by Figure 16, which shows one computation with the temperature gradient effects included and a second computation for which the partition coefficients and diffusivities were constant and chosen at the mean temperature level in the channel. The difference between the two computations is not too large and indicates that simpler and less time-consuming computations using the input variables at the mean temperature in the channel should be adequate for engineering design and evaluation of the respirator performance. Closer agreement for the two cases would result if the constant property values were selected at temperatures somewhat above the mean values.

Comparison with experiment

One of the difficulties in assessing the limitations of the

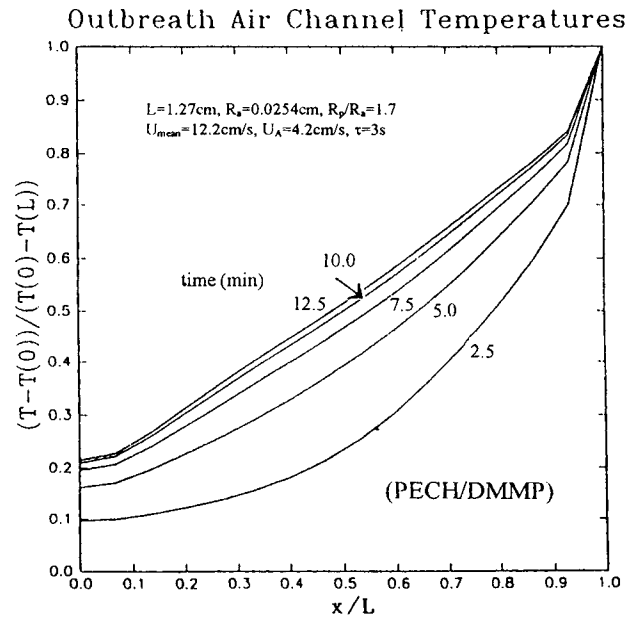

Figure 14. Predicted temperature distributions in the air channel during breathing at selected times.
The system reaches equilibrium quite rapidly.

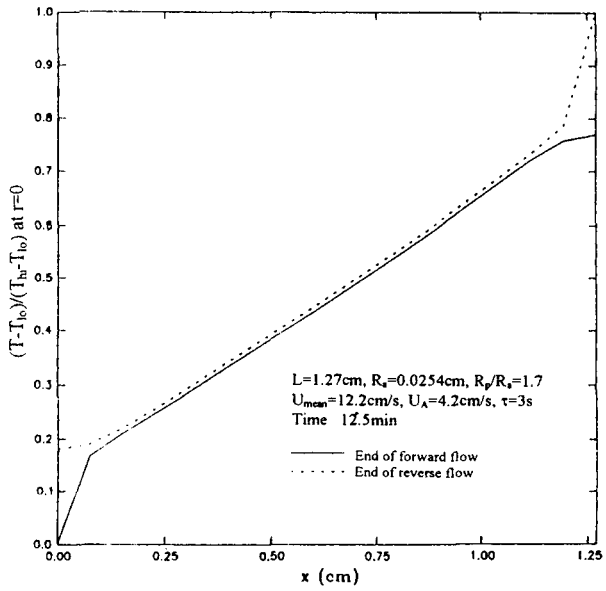

Figure 15. Temperature distribution following in and out breaths after 12.5 min of respiration.

numerical model is that of accurately determining the necessary property values (partition coefficient and diffusivity of the gas in both the polymer and in air—all of which are temperature dependent) at the low concentrations of interest. In addition, gas-concentration measurements in the simulated breathing experiments described below were found to be very susceptible to error at the low concentrations considered. (For example, the value of C_0 for DMMP was typically of the order of 0.1 torr, and values of C_m at the mouth, $x = L$, of much less than C_0 were sought.) These difficulties and uncertainties are detailed in Brown et al. (1996a). Thus it is difficult to determine the absolute accuracy of the numerical model results. However, as shown below, and by the parametric study presented earlier, the model at the very least provides useful guidance, can serve as a screening tool, and predicts trends including the nonlinear influence of parameters such as tube length and velocity. In addition, as shown below, the model is conservative in that the experiments show better performance (lower concentrations at the mouth) than the numerical predictions.

Simulated breathing tests. A series of simulated breathing tests were conducted in a simulated breathing loop described in detail in Brown et al. (1996a,b). Breathing flows were driven by a pair of bellows pumps that delivered a controlled volumetric flow that varied sinusoidally with time. Contaminant gas was introduced using a bubbler system to provide feed at a preset concentration within a nitrogen carrier gas. Multichanneled polymer test modules simulating sections of a respirator were exposed to this feed flow. On out-breath the bellows delivered gas (nitrogen) of controlled humidity and temperature back through the test module. Flame ionization detectors (FIDs) were used to measure the inlet and exit (mouth) contaminant concentrations. Detailed results of these experiments can be found in Brown et al. (1996a,b). Only a limited amount of experimental data is presented here for validation of the numerical predictions.

Figure 17 compares results of numerical simulations with experimental data for the case of a 1.27-cm-long DMS module composed of 414 holes ($R_a = 0.025$ cm) at a breathing rate of 10/min exposed to DMMP gas contaminant at a concentration of 15% of the saturated value. Results are presented as the ratio of the concentration measured at the mouth C_m (at $x = L$) to the input concentration, C_o, as a function of time. Three sets of experiments that provide a measure of experimental repeatability are shown. At 2 h of breathing, the variation is about 30% about the mean value,

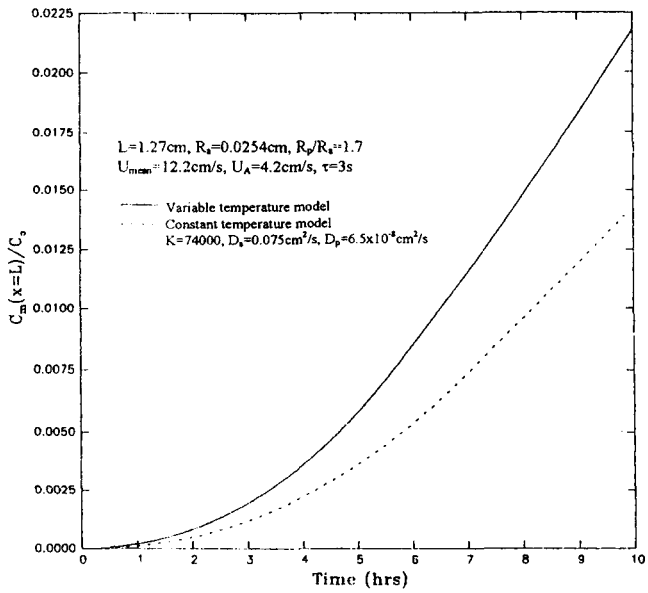

Figure 16. Results obtained with temperature effect included vs. those using an average constant temperature.

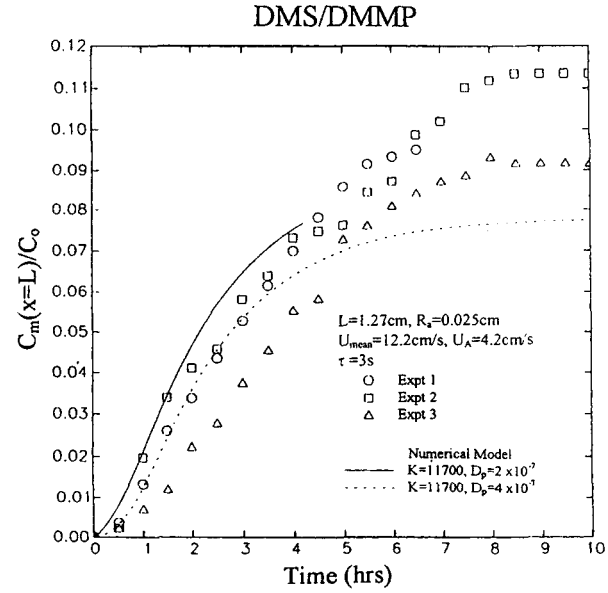

Figure 17. Simulated breathing test repeated three times for a DMMP/DMS module.

Data Repeated are compared with numerical predictions.

while at 8 h, the variation is about ±5% about the mean. These are compared with the results of two numerical simulations of this case denoted by the solid and dashed lines. These were run for a measured value of $K = 11{,}700$ (Brown et al., 1996a), and for two values of the polymer diffusivity, D_p, the lower value corresponding to the measured value. Both simulations are seen to compare well with the overall levels of the experimental data except at long times. The higher diffusivity calculation is seen to be a better short-term match to the data, while the lower diffusivity case is seen to better predict the longer-term performance. Of significance is the fact that the experimentally measured concentrations at the mouth are lower than those predicted by the model, resulting in better respirator performance than that predicted. This is a general trend that has been observed in comparing all experimental and numerical results. The difference is generally most pronounced at short times.

Figures 18 compares predictions with data from DMS modules of tube radius 0.079 cm and lengths of both 1.27 and 2.54 cm exposed to DMMP. Data from two runs with the longer module are presented and are seen to exhibit very good repeatability. The nonlinear nature of the response with tube length is apparent. At 4 h of breathing, the shorter module produces a concentration of 10% of C_o. However, doubling the module length cuts the measured concentration at 4 h to 0.4% of C_o—a factor of 25 reduction in measured concentration. Comparison of predicted and measured performance for the shorter module is seen to be quite good. However, the model is seen to significantly underpredict performance for short times for the long module.

The overprediction of concentrations at the mouth by the model, particularly at early times, may be due to concentration-dependent effects not included in the model in which the value of the partition coefficient increases at very low concentrations. Such behavior is often observed in both absorption and adsorption phenomena.

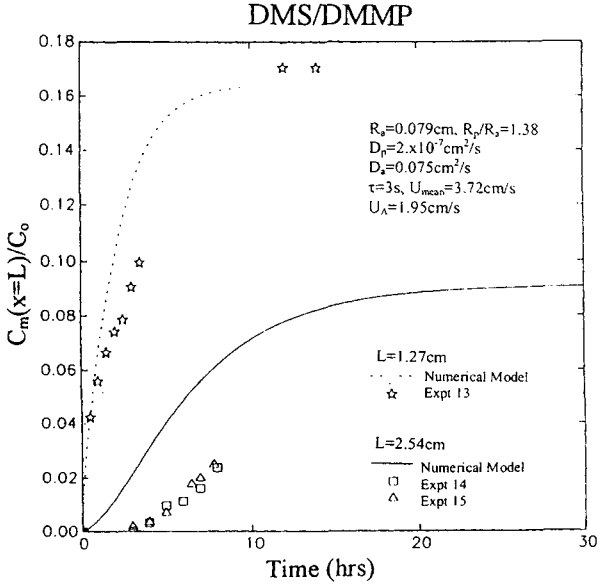

Figure 18. Effect of module length.

Comparison of experimental data and numerical predictions for a factor of 2 variation in length.

Influence of Concentration-dependent Partition Coefficient. To check the plausibility of a concentration dependence of the partition coefficient at low concentrations, a simple nonlinear variation of the partition coefficient K was assumed and utilized in the numerical model:

$$K = \frac{K_o}{\left(\frac{K_o}{K^*} - 1\right)\left(\frac{C}{C^*}\right) + 1}, \qquad C \le C^*, \tag{25}$$

$$K = K^*, \qquad C \ge C^*. \tag{26}$$

In this relation, the value of K is independent of the concentration and equal to K^* for values of the concentration larger than C^*, and rises smoothly with decreasing concentration to K_o, the value at zero concentration. The results of simulations are presented in Figure 19 for two cases: $K_o/K^* = 2$ and 5. In both cases the value of C^* was taken equal to the minimum value at which K was obtained experimentally (10% of saturation corresponding to 0.65 C_o in the experiments), and $K^* = 11{,}700$. Figure 19 shows the simulations together with the calculation for constant K and experimental data. As can be seen, the use of this concentration-dependent partition coefficient results in predictions that more closely agree with experimental data at short times. Since the selection of the variation of K was arbitrary, one could expect that closer correspondence with a better expression of the actual variation of K with C has not been measured. In addition, as pointed out by one of the revisions, K is expected to decrease further in the presence of moisture.

Implications for respirator design

The advantage of employing two-way breathing over the conventional one-way breathing is illustrated in Figure 20, which compares results of simulations of both cases in terms of the concentration at the mouth as a function of time. As can be seen in this figure, concentrations at the mouth are

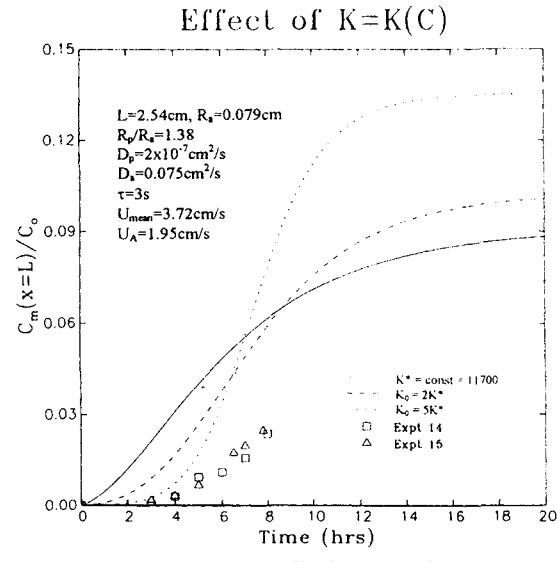

Figure 19. Numerical predictions using concentration-dependent partition coefficients vs. experimental data for DMMP/DMS.

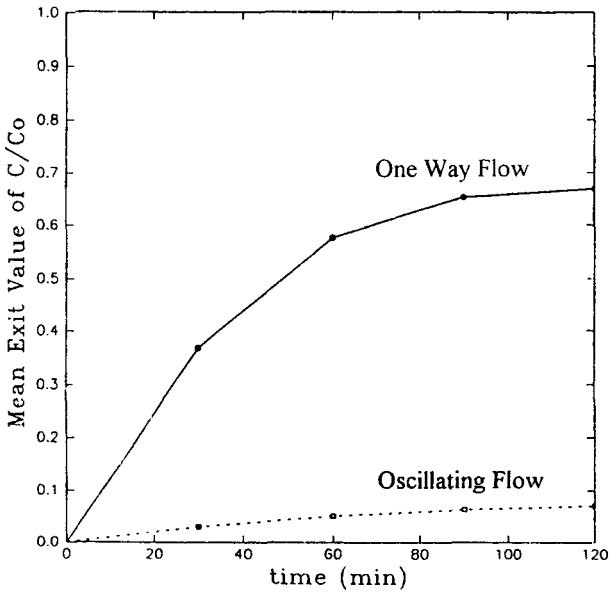

Figure 20. Concentration ratios at the mouth with and without oscillatory flow.

$R_a = 0.254$ cm; $L = 1.27$ cm; $K = 10^4$; $U_{mean} = 15$ cm/s; $D_p = 10^{-7}$ cm^2/s; $D_a = 0.075$ cm^2/s.

reduced by at least an order of magnitude by employing two-way breathing. These order of magnitude concentration reductions have also been observed experimentally (Brown et al., 1996a,b).

The concept envisioned a porous absorbent polymer material formed in the manner of a surgical mask, through which breath is both inhaled and exhaled. The absorbent polymer would constitute the major weight of the respirator. Its value can be expressed by the relation

$$\textit{Polymer Weight} = \rho_p LA(1-\epsilon), \tag{27}$$

where A is the total face area of the filter and ϵ is the fraction of A occupied by the channel holes. For holes placed at the corners of equilateral triangles

$$\epsilon = \frac{\pi}{2\sqrt{3}}\left(\frac{R_a}{z}\right)^2 = \left(\frac{R_a}{R_p}\right)^2. \tag{28}$$

For a given mean respiration volumetric flow rate, Q (typically 30 to 40 L/min), the face area, A, and the mean apparent flow velocity, U_A, are related by

$$Q = U_A A, \tag{29}$$

and in terms of the channel velocity,

$$U_{\text{mean}} = A\epsilon. \tag{30}$$

Combining the preceding relations, we get for the polymer weight

$$\text{Polymer Weight} = \rho_p QL\left(\frac{R_p^2}{R_a^2} - 1\right)/U_{\text{mean}}. \tag{31}$$

For a desired performance specified by the breakthrough time to reach a limiting exit concentration of toxic gas, the analyses and tests described earlier show the desirability of low mean velocity and long channel lengths, whereas low weight, as seen in Eq. 31, requires just the opposite. The performance of the filter is also dependent on the polymer and gas properties, partition coefficient, and diffusivity, as well as the channel hole radius and spacing. The favorable effect of small channel dimensions is limited by the requirements of low breathing resistance. For the channels of interest in respirators, the Reynolds numbers of the flows are so small (less than 10) that fully developed laminar flow is to be expected. The pressure loss in breathing can therefore be expressed by the following relation:

$$\Delta p = 8\mu U_{\text{mean}} L/R_a^2, \tag{32}$$

in which μ is the viscosity of the air. From this expression, values of U_{mean} of 24 cm/s, radii of 0.0254, cm, and channel lengths of 5 cm will produce a pressure loss of approximately 3 mm of water. Somewhat higher pressure loss can easily be sustained and would allow reductions in channel diameters with their favorable effect on performance. The Mine Safety and Health Administration suggests pressure losses at 85 L/min of 60 mm of water as being reasonable for pesticide respirators. For this level of loss, the tube radius in the cited example could be reduced from 0.0254 cm to 0.0057 cm.

The study results clearly point to the desirability of identifying polymers with very high partition coefficients for target gases. For example, Figure 6, discussed earlier, predicts two orders of magnitude lower exit concentrations at 4 h of operation in going from a value of $K = 11{,}700$ to $K = 80{,}000$, approximately a factor of 7 increase. Less critical, but still important, is high diffusivity in the polymer (see Figure 7), which enables effective use of a thicker layer of polymer, increasing the amount of gas that can be absorbed. Thus, from a practical standpoint, development of polymers with very large K and high diffusivities is desired.

From a design standpoint, the results demonstrate the desirability of operating in the early time region prior to saturation, such that the highly nonlinear relation between length, polymer thickness, and velocity can be exploited. The results clearly point to the importance of minimizing passage diameter to decrease radial diffusion resistance. Thus, a desirable system design would incorporate many small-diameter passages whose lengths are long relative to their diameters and whose polymer thickness is sized to achieve the desired level of gas removal at the desired time.

Conclusions

From a numerical study of breathing in and out through polymer-lined channels, the following general conclusions can be reached:

1. Relative to direct one-way flow through the channels, there is an order of magnitude increase in the time to reach any specified exiting concentration.

2. The oscillating flow system reaches a final equilibrium value of the exiting concentration at a fraction of the entering concentration, which is not possible with a one-way flow system.

3. The temperature distribution in the polymer is linear from the entrance of the channel to the exit at the mouth, varying from ambient atmospheric temperature to body temperature. Use of an average temperature can approximate performance, but underpredicts the exit concentrations by approximately 25%. Due to the typical decrease in partition coefficient with temperature, the effectiveness of the absorption system decreases with increasing temperature.

4. Polymer gas pair partition coefficients are of primary importance in maximizing breakthrough time to a limiting concentration. The model predicts very strong influence of the partition coefficient. This points to the need of identifying polymers with very high partition coefficients. The model also demonstrates the desirability of high diffusivities in the polymer. This enables utilization of thicker polymer coatings to absorb more gas.

5. Performance of a channeled polymer filter is nonlinear with regard to increases in length or decreases in velocity, particularly at times well before reaching an equilibrium. Halving the apparent velocity or doubling the length results in an order-of-magnitude decrease in concentration at the mouth.

6. Numerical simulations were shown to predict the trends of the experimental data. However, experiments were found to consistently produce lower concentrations than those predicted, particularly at short times.

7. Two-way breathing using polymeric absorption is predicted to be promising for respirator use when employed with materials having high partition coefficients.

8. The presence of a concentration-dependent partition coefficient, such that the partition coefficient increases at low concentrations, is predicted to significantly improve polymer absorption and decrease concentrations exiting the tube, particularly at early times.

Acknowledgments

The work was performed at DYNAFLOW, Inc., in Fulton, MD, under SBIR Grant R440H03011-33 from the National Institute of Occupational Safety and Health. The authors wish to thank several colleagues at DYNAFLOW for many helpful discussions and suggestions during the course of this work.

Literature Cited

American Conference of Governmental Hygienists, "Threshold Limit Values and Biological Exposure Indices for 1989-1990," Cincinnati, OH (1989).

Brown, C., K. Kalumuck, S. Prabhukumar, and G. Chahine, "Development of a Two-way Breathing Respirator with Polymeric Absorption," Tech. Rep. 93001-3(NIOSH Phase II SBIR, DYNAFLOW, Inc., Fulton, MD (1996).

Brown, C., K. Kalumuck, and G. Frederick, "An Experimental Study of Oscillating Flow for Use in Respirators," *Amer. Ind. Hygiene J.* (1996).

Grate, J., A. Snow, D. Ballantine, H. Wohltjen, M. Abraham, R. McGill, and P. Sasson, "Determination of Partition Coefficients from Surface Acoustic Wave Vapor Sensor Responses and Correlation with Gas-Liquid Chromatographic Partition Coefficients," *Anal. Chem.*, **60**, 869–875 (1988).

Hagel, D., V. Laverty, and C. Brown, "A Basic Research Study of Factors Affecting the Collection Efficiency and Power Use of High Volume Sampling Systems," Hydronautics, Inc. Tech. Rep. 7413-1, Hydronautics, Inc., Laurel, MD (1977).

Kalumuck, K., C. Brown, S. Prabhukumar, G. Chahine, G. Frederick, and P. Aley, "Staged Gas Concentration Amplification of Gases Using Polymer Absorbers," Tech. Rep. 94002-1, DYNAFLOW, Inc., Fulton, MD (1994).

Peyret, R., and T. Taylor, *Computational Methods for Fluid Flow*, Springer-Verlag, New York (1983).

Tollen, E. D., "Sorption Properties of Activated Carbon," *Comprehensive Progress Rep.—Contract DA18-035-AMC-10953(A)*, Edgewood Arsenal, MD (1968).

White, F. M., *Viscous Fluid Flow*, McGraw-Hill, New York (1974).

Yaws, C. L., B. Li, and S. Nijhawan, "Adsorption-Capacity Data for 283 Organic Compounds," *Environ. Eng. World*, (May/June 16, 1995).

Manuscript received May 8, 1996, and revision received May 12, 1997.